PHYSICAL REVIEW D **86,** 074027 (2012)

Production of χ_b mesons at the LHC

A. K. Likhoded,* A. V. Luchinsky,† and S. V. Poslavsky‡
Institute for High Energy Physics, Protvino 142284, Russia
(Received 16 April 2012; published 22 October 2012)

In the present paper we discuss the P-wave bottomonium production within both color octet and color singlet models in next-to-leading order at LHC energies. We calculate the cross section and the transverse momentum distributions for the $\chi_{1,2b}$ states. We obtain that the ratios of bottomonium and charmonium spin state production are fundamentally complementary at different p_T scales. We give predictions for the ratio of the $n = 2$ and $n = 1$ radial excitations production cross sections.

DOI: 10.1103/PhysRevD.86.074027 PACS numbers: 14.40.Pq, 13.85.−t, 14.40.Nd

I. INTRODUCTION

Studies of heavy quarkonia give a deeper understanding of the quantum chromodynamics. In the recent measurements made by ATLAS [1] and D0 [2] Collaborations the new data for the $b\bar{b}$ systems were obtained. The radial excitation of the P-wave χ_b states was observed in radiative transitions to the S-wave Υ states, while $\chi_b(3P)$ was seen for the first time. The χ_b system is a triplet of closely spaced states with total spin $J = 0$, 1, and 2 that were not yet observed separately at ATLAS. Usually, only 1^{++} and 2^{++} can be detected, since the 0^{++} state has a very small radiative branching fraction. So, in the present paper, we shall focus on the production of 1^{++} and 2^{++} charmonium and bottomonium states. We shall consider the production with high transverse momentum of the final quarkonium.

The main contribution to the production processes at high energies ($\sim$ tera-electron-volt) is given by gluon-gluon subprocesses. The problem of the quarkonia production can be divided into two parts. The first part of the problem is to obtain the nonzero transverse momentum of the final quarkonia using the integrated partonic distributions. The second part consists in the hadronization process, i.e., formation of the quarkonia with certain quantum numbers. For example, let us consider the production of the $|^3S_1\rangle$ (1^{--}) state. The colorless state with such quantum numbers cannot be produced from two gluons because of the charge parity conservation. So, the production of the color singlet state with the additional emission of a gluon in the final state was introduced [3,4] to explain the quarkonia production. Additional emission of the gluon gives the p_T distribution and removes the prohibition of the 1^{--} state production. It is well known that such a model, in its naive understanding, is in contradiction with the experimental data at high p_T. In the case of P-wave meson production the situation is different: 0^{++} and 2^{++} states can be produced from two gluons, but in the collinear approximation (with integrated over p_T partonic distributions) the transverse momentum distribution of final quarkonium cannot be obtained. Moreover, the $|^3P_1\rangle$ state cannot be produced because of the Landau-Yang theorem, which forbids the production of an axial meson from two massless gluons. These problems have led to the approach, known as k_T factorization [5–8], in which unintegrated partonic distributions are used. However, we think that such an approach should play a significant role at the low p_T region only, while in the high p_T region the dominant contribution to the p_T is given by the processes with the emission of a single hard gluon in the final state.

In this paper we try to resolve the above problems by considering a set of diagrams, in which high p_T is achieved by the emission of single hard gluon, mostly from the initial state. It turns out that all three P-wave states, including 1^{++} are allowed. As we shall see, the color-singlet contributions give p_T dependence, which is similar to the experimental data for χ_c mesons, for example, from CDF [9], but the absolute normalization of the cross section is several times smaller than in the experiment. To resolve this contradiction we took into account the color-octet contributions to the cross sections. In the next section we show that if we consider the color-octet matrix elements as free parameters, the good agreement with the experimental data can be obtained for the case of χ_c, and the predictions for the χ_b states can be provided. Next, we consider the cross section ratio of 2^{++} and 1^{++} production for both χ_c and χ_b, which was recently measured for charmed mesons at the LHCb detector [10] and shows that our approach gives the value, lying at the lower limit of uncertainties of the LHCb data. There are no such experimental data on the bottomonium production yet, and our result should be considered as the theoretical predictions for further experiments. Next, we consider the ratio of the $n = 2$ and $n = 1$ radial excitations, which is not measured yet, and present our theoretical predictions.

II. χ_c PRODUCTION AT HIGH p_T

The cross section of heavy quarkonium production in hadronic interaction can be expressed through the cross sections of hard subprocesses:

*Anatolii.Likhoded@ihep.ru
†Alexey.Luchinsky@ihep.ru
‡stvlpos@mail.ru

$$d\sigma[pp \to \mathcal{Q} + X] = \int dx_1 dx_2 f_g(x_1; Q) f_g(x_2; Q) d\hat{\sigma}[\mathcal{Q}]. \quad (1)$$

Here, $\mathcal{Q}$ is one of the $|^3P_J\rangle$ states, $x_{1,2}$ are the momentum fractions of the partons, $f_g(x_{1,2}; Q)$ are the gluon distribution functions in initial hadrons, and $d\hat{\sigma}[\mathcal{Q}]$ is the cross section of the meson production at the partonic level.

As already mentioned in the Introduction, to obtain the nonzero transverse momentum of final quarkonia using the usual partonic distributions, it is necessary to consider next-to-leading-order subprocesses with the emission of an additional gluon, i.e., $gg \to \chi_{bJ} g$. The corresponding Feynman diagrams are shown in Fig. 1. The partonic cross sections of these reactions were calculated by a number of authors [11–14], but results presented in Ref. [13] disagree with the other works. The reason is that diagrams shown in Fig. 1 include the 3-gluon vertex and the additional ghost contributions should be included. Our calculations performed in QCD axial gauge (which does not require additional ghost contributions) reproduces the results of Refs. [11,12,14].

It should be noted that the above expressions depend on two scale parameters: the renormalization scale μ in strong coupling constant $\alpha_S(\mu)$ and the maximum transverse momentum of collinear gluons Q in structure functions $f(x, Q)$. At low energies the variation of these scale parameters leads to significant variation of the total cross sections [15], while for the energies about several tera-electron-volts the dependence is not crucial. In our work we will use the value $Q = \mu = M$, where M is the mass of the heavy quarkonium. Also we shall neglect the mass difference between states from the same $\chi_J(nP)$ triplet.

It is known that the color-singlet model of $q\bar{q}$ pair hadronization into an observable meson does not fully describe experimental data. The reason is that the color-singlet model is only the first approximation in the Fock structure of the quarkonium state [16]:

$$\begin{aligned}|^{2S+1}L_J\rangle = {} & O(1)|^{2S+1}L_J{}^{[1]}\rangle \\ & + O(v)|^{2S+1}(L \pm 1)_{J'}{}^{[8]}g\rangle \quad \text{(E1)} \\ & + O(v^2)|^{2(S\pm1)+1}L_{J'}{}^{[8]}g\rangle \quad \text{(M1)} \\ & + O(v^2)|^{2S+1}L_J{}^{[1,8]}gg\rangle \quad (\text{E1} \times \text{E1}) + \ldots,\end{aligned} \quad (2)$$

where v is the relative velocity of quarks in heavy quarkonium. In the above expression E1 and M1 are electric ($\Delta L = 1$, $\Delta S = 0$) and magnetic ($\Delta S = 1$, $\Delta L = 0$) transitions, respectively. In the case of χ_c mesons Eq. (2) gives

$$\begin{aligned}|\chi_{cJ}\rangle = {} & \langle \mathcal{O}^{\chi_{cJ}}[^3P_J^{[1]}]\rangle |^3P_J{}^{[1]}\rangle \\ & + \langle \mathcal{O}^{\chi_{cJ}}[^3S_1^{[8]}]\rangle |^3S_1{}^{[8]}\rangle + \langle \mathcal{O}^{\chi_{cJ}}[^1P_1{}^{[8]}]\rangle |^1P_1^{[8]}\rangle \\ & + \sum_{J'} \langle \mathcal{O}^{\chi_{cJ}}[^3P_{J'}^{[8]}]\rangle |^3P_{J'}{}^{[8]}\rangle + \ldots.\end{aligned} \quad (3)$$

Here the first two terms are of order $O(v)$, and the next two terms are of order $O(v^2)$.

In Fig. 2 the contributions from different states in (3) to the p_T distributions of J/ψ mesons produced via χ_c radiative decays,

$$\begin{aligned}\frac{d\sigma}{dp_T}[p\bar{p} \to \chi_c + X \to J/\psi + X] = {} & \mathrm{Br}[\chi_{c1}]\frac{d\sigma}{dp_T}[p\bar{p} \to \chi_{c1} + X] \\ & + \mathrm{Br}[\chi_{c2}]\frac{d\sigma}{dp_T}[p\bar{p} \to \chi_{c2} + X],\end{aligned}$$

which are shown in comparison with the CDF experimental data [9]. The octet $|^3S_1^{[8]}\rangle$ state gives p_T distribution

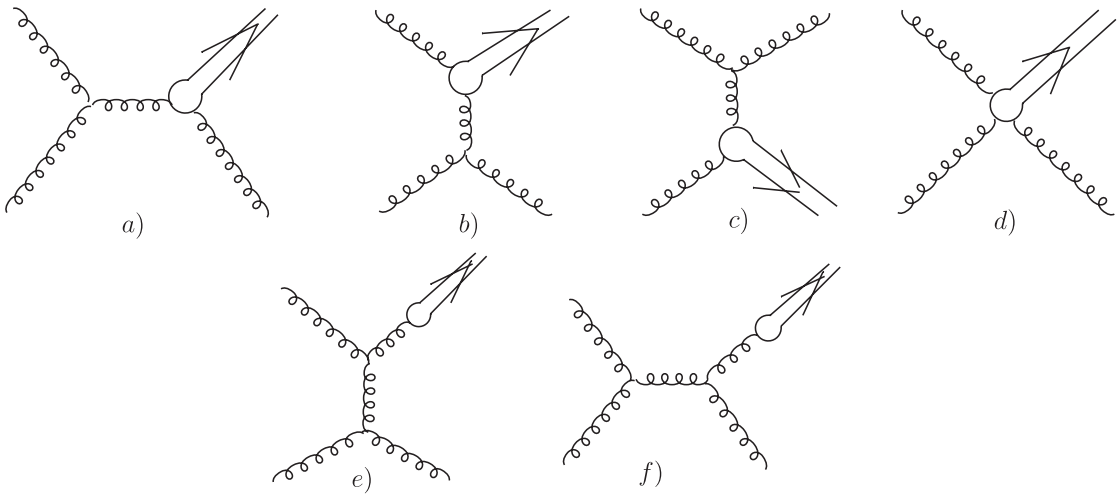

FIG. 1. The Feynman diagrams of the $gg \to \chi_b g$ subprocesses. The first four diagrams are valid for both color-singlet and color-octet mechanisms, while the last two diagrams correspond to the octet production only.

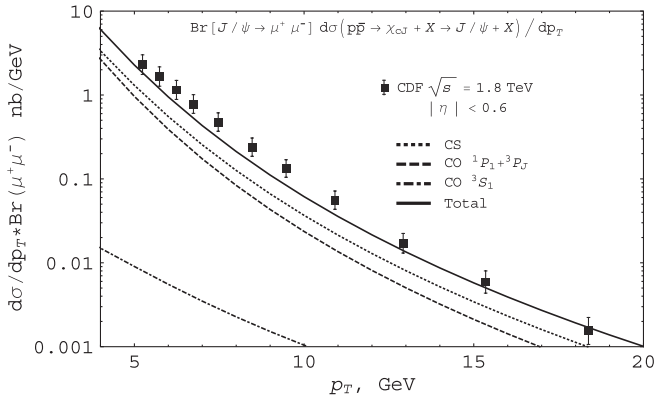

FIG. 2. Contributions to the χ_c production from different states. Dotted line is color-singlet contribution. Dashed line is a contribution from the octet $|^3P_J^{[8]}\rangle$ and $|^1P_1^{[8]}\rangle$ states. Dot-dashed line is color-octet $|^3S_1^{[8]}\rangle$ state contribution. Solid line is a sum over all contributions. Experimental points are taken from CDF report [9].

approximately described by $\sim 1/p_T^4$, which is far different from the experimental one, which, in turn, is approximately described by $\sim 1/p_T^6$. So, to fit the experimental data, we should assume that $|^3S_1^{[8]}\rangle$ gives a negligibly small contribution in the considered p_T interval and plays a role for higher p_T only. The other states from the Fock expansion (3), including color singlet, have the p_T distribution similar to the experimental measurement. To fit the experimental data, we used CDF data for the χ_c production and the available data for the cross-section ratio of $\sigma(\chi_{c2})/\sigma(\chi_{c1})$ [10,17,18] (see next section and Fig. 4). The singlet contribution is determined by the singlet matrix element $\mathcal{O}[^3P_J^{[1]}]$, which is connected with the derivative of the radial part of the wave function at the origin:

$$\langle \mathcal{O}^{\chi_{cJ}}[^3P_J^{[1]}]\rangle = \frac{3}{4\pi}(2J+1)|R'(0)|^2.$$

For the last one we took the value derived from the χ_{c2} photonic width in leading order:

$$|R'(0)|^2 = 0.075\ \text{GeV}^5.$$

The octet matrix elements for $|^3S_1^{[8]}\rangle$ satisfy the multiplicity relations

$$\langle \mathcal{O}^{\chi_{cJ}}[^3S_1^{[8]}]\rangle = (2J+1)\langle \mathcal{O}^{\chi_{c0}}[^3S_1^{[8]}]\rangle.$$

For the last one we obtained from our fit the following value:

$$\langle \mathcal{O}^{\chi_{c0}}[^3S_1^{[8]}]\rangle \lesssim 2\times 10^{-5}\ \text{GeV}^3. \quad (4)$$

Since $|^1P_1^{[8]}\rangle$ and $|^3P_J^{[8]}\rangle$ states have similar p_T dependence, they could not be resolved separately, and only a linear combination of the corresponding octet matrix elements can be determined. In the notations of Ref. [14] we obtain the following values for the nonperturbative parameters:

$$\langle R^{\chi_{c0}}[^1P_1^{(8)}]\rangle = \langle R^{\chi_{c0}}[^3P_{J'}^{(8)}]\rangle = 0.01\ \text{GeV}^5. \quad (5)$$

The last result is independent of J'. Taking into account the statistical weight of the χ_{cJ} state, the corresponding parameters for the χ_{cJ} production can be recovered:

$$\langle R^{\chi_{cJ}}[^1P_1^{(8)}]\rangle = (2J+1)\langle R^{\chi_{c0}}[^1P_1^{(8)}]\rangle,$$
$$\langle R^{\chi_{cJ}}[^3P_{J'}^{(8)}]\rangle = (2J+1)\langle R^{\chi_{c0}}[^3P_{J'}^{(8)}]\rangle.$$

At this point we need to discuss the results of our fit. In most works (see, for example, review Ref. [19]) it is acceptable to neglect the P-wave octet contributions because of the velocity power counting rules, and the following ranges of values of the nonperturbative matrix element for the $|^3S_1^{[8]}\rangle$ state are considered:

$$\langle \mathcal{O}^{\chi_{c0}}[^3S_1^{[8]}]\rangle \sim (0.1\text{–}0.5)\times 10^{-2}\ \text{GeV}^3.$$

Nevertheless, we state that the $|^3S_1^{[8]}\rangle$ contribution gives inappropriate p_T dependence to describe the experimental data, and therefore octet P-wave contributions should be included.

On the other hand, the nonperturbative value of the octet $|^3S_1^{[8]}\rangle$ contribution from work [8] is closer to our result:

$$\langle \mathcal{O}^{\chi_{c0}}[^3S_1^{[8]}]\rangle \sim 2\times 10^{-4}\ \text{GeV}^3,$$

but the derivative of the radial part of the wave function at the origin is about several times bigger than ours:

$$|R'(0)|^2 \sim 0.37\ \text{GeV}^5,$$

so the almost entire contribution is given by the singlet term. We think that this value is unreasonably high and does not agree with experimental data. A possible reason for the contradiction is that authors derive this value from the photonic width including the QCD radiative correction. It is clear that by using such an approach the radiative corrections to the initial state production should be considered on a par with radiative corrections in the final state, but this was not performed.

III. χ_b PRODUCTION AT HIGH p_T

Let us proceed to the χ_b mesons production. The picture of the bottomonium production is almost the same as in the charmonium case. The only difference is that probabilities in Fock expansion (3) have different values. We shall assume that relative contributions from different Fock states are similar to charmonium mesons and do not depend on the radial excitation number n. So, for example,

$$\frac{\langle \mathcal{O}[^3P_J^{[8]}\to\chi_c]\rangle}{\langle \mathcal{O}[^3P_J^{[1]}\to\chi_c]\rangle} = \frac{\langle \mathcal{O}[^3P_J^{[8]}\to\chi_b(nP)]\rangle}{\langle \mathcal{O}[^3P_J^{[1]}\to\chi_b(nP)]\rangle}. \quad (6)$$

From the dimension analysis, it is clear that

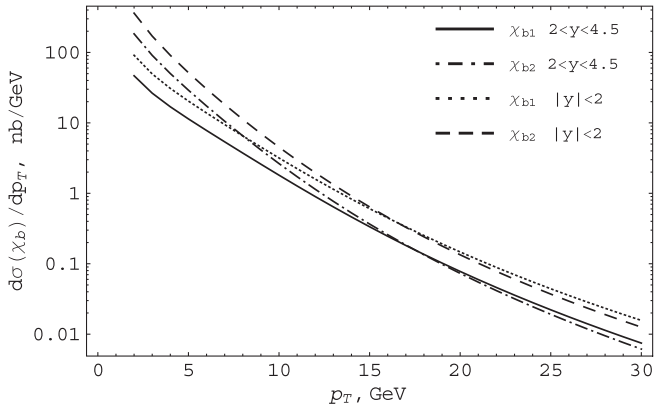

FIG. 3. Transverse momentum distributions of the χ_{b1} and χ_{b2} mesons at $\sqrt{s} = 8$ TeV. The derivative of the wave function at the origin is $|R'_n(0)|^2 = 1$ GeV^5, which is in agreement with potential models, presented in Table I. Other nonperturbative parameters were obtained in the previous section in the case of charmonium and corresponds to the total curve in Fig. 2 and then evaluated for bottomonium using (6) and (7).

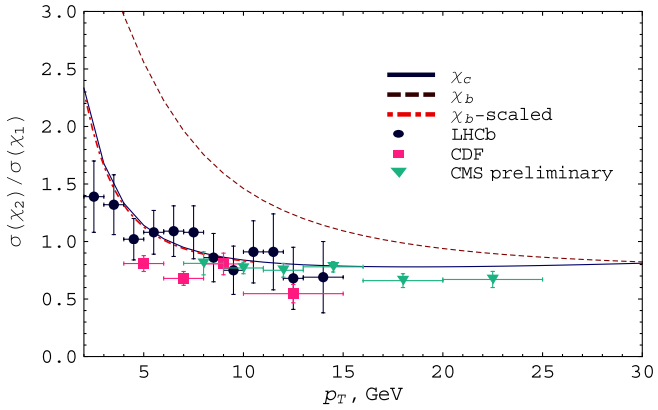

FIG. 4 (color online). Transverse momentum distributions of the $d\sigma[\chi_2]/d\sigma[\chi_1]$ ratio. Solid and dashed lines stand for charmonium and bottomonium mesons. The dot-dashed line corresponds to the rescaled bottomonium ratio: $\sigma_{b2}/\sigma_{b1}(M_{\chi_c}/M_{\chi_b}p_T)$. As it is seen, it almost matches the charmonium curve. The experimental results for charmonium from LHC [10] are shown with dots, CDF [17]—with rectangles, and CMS [18]—with triangles.

$$\frac{\langle \mathcal{O}[^3S_1^{[8]}]\rangle}{\langle \mathcal{O}[^3P_J^{[1]}]\rangle} \sim \frac{1}{M^2}.$$

So, for $|^3S_1\rangle$ we take

$$\frac{\langle \mathcal{O}[^3S_1^{[8]} \to \chi_c]\rangle}{\langle \mathcal{O}[^3P_J^{[1]} \to \chi_c]\rangle} = \frac{M^2_{\chi_b}}{M^2_{\chi_c}} \frac{\langle \mathcal{O}[^3S_1^{[8]} \to \chi_b(nP)]\rangle}{\langle \mathcal{O}[^3P_J^{[1]} \to \chi_b(nP)]\rangle}. \quad (7)$$

In Fig. 3 we show our results for the transverse momentum distributions for axial and tensor bottomonium. For the derivative of the wave function at the origin we take

$$|R'_n(0)|^2 = 1 \text{ GeV}^5,$$

which is in agreement with potential models, presented in Table I. For other nonperturbative parameters we use values obtained in the previous section and evaluated with (6) and (7). Presented curves allow one to easily reconstruct the distributions for any $|R'_n(0)|$ value by simply multiplying with the corresponding factor from Table I.

In Fig. 4 the p_T dependence of the $\chi_Q(J=2)/\chi_Q(J=1)$ ratio is depicted. In the case of charmonium mesons we compare our results with the LHCb data [10], CDF data [17], and CMS preliminary [18]. For both $(c\bar{c})$ and $(b\bar{b})$ mesons we present the cross-section ratio in the rapidity range $2 < y < 4.5$, but it is clear that this ratio depends weakly on the rapidity cut, so these predictions should also be valid for other rapidity regions. One can easily see that within the experimental errors our results for charmonia agree well with experiment, so the approach used in our paper is valid. It is clear that since the cross section is proportional to $|R'(0)|^2$ and if the mass gap between $\chi_J(nP)$ states with different radial numbers n is neglected, the ratio $d\sigma[\chi_2(nP)]/d\sigma[\chi_1(nP)]$ does not depend on n and curves for charmonia and bottomonia presented in Fig. 4 are universal.

One interesting property can be seen from Fig. 4: the bottomonium curve matches the charmonium curve if we perform the rescaling of the p_T variable: $p_T \to (M_{\chi_c}/M_{\chi_b})p_T \approx (1/3)p_T$. Moreover, this fact is an exact model-independent theoretical result, which can be obtained from the dimension analysis. Indeed, the cross section of the quarkonia production depends on three dimensional parameters: hadronic energy, transverse momentum of final quarkonium, and its mass:

$$\frac{d\sigma_J}{dp_T} \equiv \frac{d\sigma_J}{dp_T}(s, p_T, M).$$

The cross-section ratio $J = 2$ and $J = 1$ is a dimensionless function of these parameters. Hence, we can write

$$\frac{d\sigma_2(z^2 s, zp_T, zM)}{dp_T} \Big/ \frac{d\sigma_1(z^2 s, zp_T, zM)}{dp_T} = \frac{d\sigma_2(s, p_T, M)}{dp_T} \Big/ \frac{d\sigma_1(s, p_T, M)}{dp_T}. \quad (8)$$

Taking $M = M_{\chi_c}$ and $z = M_{\chi_b}/M_{\chi_c}$, we obtain

TABLE I. $|R'_{nP}(0)|^2$ (in GeV^5) from different potential models.

	[20]	[21]	[22]	[23]	[24]	[25]
$\chi_b(1P)$	0.71	1.02	2.03	0.94	0.84	0.51
$\chi_b(2P)$	0.99	0.88	2.2	1.13	0.98	0.25
$\chi_b(3P)$	...	...	2.43	1.17	1.03	...

$$\frac{d\sigma_{b2}(zp_T;s)}{dp_T}\Big/\frac{d\sigma_{b1}(zp_T;s)}{dp_T} = \frac{d\sigma_{c2}(p_T;s/z^2)}{dp_T}\Big/\frac{d\sigma_{c1}(p_T;s/z^2)}{dp_T}. \quad (9)$$

Hence, if we know the charmonium ratio transverse momentum distribution at some c.m. energy s, we can easily reconstruct the bottomonium ratio distribution at energy $s(M_\Upsilon/M_{J/\psi})^2$. This relation is not violated by the scale dependence of α_s and partonic distributions, since they are canceled in the ratio.

It is intuitively clear that at least for high energies the ratio weakly depends on s, since both axial and tensor mesons acquire universal behavior in s, so the s dependence cancels in this ratio. This argument does not work for low s, when another partonic channel becomes significant. The value of $z \sim 3$, so the bottomonium distribution at $\sqrt{s} = 8$ TeV corresponds to the charmonium distribution at $\sqrt{s} \sim 2.6$ TeV, which is still very high, so the gluonic subprocess dominates. We can expect that (9) can be approximately rewritten for high energies:

$$\frac{d\sigma_{b2}(zp_T;s)}{dp_T}\Big/\frac{d\sigma_{b1}(zp_T;s)}{dp_T} = \frac{d\sigma_{c2}(p_T;s)}{dp_T}\Big/\frac{d\sigma_{c1}(p_T;s)}{dp_T}. \quad (10)$$

A. Radial excitations

Let us now discuss the production of excited χ_b mesons at LHC. Recently $\chi_b(1P)$, $\chi_b(2P)$, and $\chi_b(3P)$ mesons were observed in $\Upsilon(1S)\gamma$ and $\Upsilon(2S)\gamma$ modes by the ATLAS [1] and D0 [2] Collaborations. In these experiments the radial excitation of the P-wave χ_b states was observed in the radiative transitions to the S-wave Υ states. Unfortunately, the exact values of the cross sections were not yet measured, but we can reconstruct them theoretically.

The experimentally observable quantities are

$$\sigma^{\rm th}[nP, mS] = \sigma^{\rm th}[pp \to \chi_b(1P) + X \to \Upsilon(mS)\gamma + X] = \sum_{J=0}^{2} {\rm Br}_J[nP, mS]\sigma_J^{\rm th}[nP], \quad (11)$$

where the following notations were used:

$$\sigma_J^{\rm th}[nP] = \sigma^{\rm th}[pp \to \chi_{bJ}(nP) + X], \qquad {\rm Br}_J[nP, mS] = {\rm Br}[\chi_{bJ}(nP) \to \Upsilon(1S)\gamma]. \quad (19)$$

The branching fractions of radiative $\chi_b(1P)$- and $\chi_b(2P)$-meson decays are known experimentally [26]:

$${\rm Br}_1[1P, 1S] = 35\% \pm 8\%,$$
$${\rm Br}_2[1P, 1S] = 22\% \pm 4\%,$$
$${\rm Br}_1[2P, 1S] = 8.5\% \pm 1.3\%,$$
$${\rm Br}_2[2P, 1S] = 7.1\% \pm 1\%,$$
$${\rm Br}_1[2P, 2S] = 21\% \pm 4\%,$$
$${\rm Br}_2[2P, 2S] = 16\% \pm 2.4\%.$$

In the case of scalar bottomonium the branching fractions are small, so we do not include them in the sum (11).

To calculate the total cross sections, we should integrate the cross-section distributions obtained in the previous section and presented on Fig. 3 over the appropriate p_T region: $\Delta < p_T < (s - M^2)/2\sqrt{s}$. We use experimental values $\Delta = 12$ GeV for ATLAS ($|y| < 2$) [1] and $\Delta = 6$ GeV for LHCb ($2 < y < 4.5$) [27]. Using these values we obtained the following prediction for the cross sections:

$$\text{(LHCb)}\ \frac{1}{|R'_n(0)|^2}\sigma^{\rm th}[\chi_{b1}(nP)] = 34.4\,\frac{\rm nb}{\rm GeV^5},$$
$$\frac{1}{|R'_n(0)|^2}\sigma^{\rm th}[\chi_{b2}(nP)] = 43\,\frac{\rm nb}{\rm GeV^5},$$
$$\text{(ATLAS)}\ \frac{1}{|R'_n(0)|^2}\sigma^{\rm th}[\chi_{b1}(nP)] = 5.2\,\frac{\rm nb}{\rm GeV^5},$$
$$\frac{1}{|R'_n(0)|^2}\sigma^{\rm th}[\chi_{b2}(nP)] = 5.6\,\frac{\rm nb}{\rm GeV^5},$$

and for the ratio $\sigma[\chi_b(2P)]/\sigma[\chi_b(1P)]$ in both cases

$$\frac{\sigma^{\rm th}[2P, 1S]}{\sigma^{\rm th}[1P, 1S]} = (0.29 \pm 0.01^{\rm th} \pm 0.1^{\rm br})\left|\frac{R'_{2P}}{R'_{1P}}\right|^2.$$

Here the first error is the error of our theoretical method, while the second is the uncertainty in the experimental values of branching fractions. This ratio is determined by the ratio of $2P$-and $1P$-state wave function derivatives at the origin (see Table I). In Table II we show the predictions of different potential models for this ratio.

In the case of $\chi_b(3P)$-meson production the corresponding branching fractions to $\Upsilon(1S)$ are not yet known, so we cannot perform a similar analysis. However, we can estimate the radiative branching fraction of the tensor meson

TABLE II. Theoretical predictions for the ratio of $\chi_b(2P)$ and $\chi_b(1P)$ production cross sections in different potential models.

Potential model	Ratio $\chi_b(2P)/\chi_b(1P)$
[20]	$0.4 \pm 0.01^{\rm th} \pm 0.14^{\rm br}$
[21]	$0.25 \pm 0.01^{\rm th} \pm 0.1^{\rm br}$
[22]	$0.32 \pm 0.02^{\rm th} \pm 0.1^{\rm br}$
[23]	$0.34 \pm 0.01^{\rm th} \pm 0.12^{\rm br}$
[24]	$0.34 \pm 0.01^{\rm th} \pm 0.12^{\rm br}$
[25]	$0.14 \pm 0.05^{\rm br}$

TABLE III. Branching fractions of $\chi_b(3P) \to \Upsilon(1S)\gamma$ decays.

Potential model	$\mathrm{Br}_2[3P, 1S]$	$\mathrm{Br}_1[3P, 1S]$
[22]	1.7%	$((41 \pm 9)\gamma - 1.3)\%$
[24]	5.4%	$((42 \pm 9)\gamma - 4.1)\%$

using the following assumptions. We assume that the main hadronic decay channel of tensor meson is 2-gluon decay,

$$\Gamma[\chi_{b2}(3P) \to gg] = \frac{128}{5}\alpha_S^2 \frac{|R_3'(0)|^2}{M^4},$$

and the radiative branching fraction of the $\chi_{b2}(3P)$ is equal to

$$\mathrm{Br}_2[3P, 1S] = \frac{\Gamma[\chi_{b2}(3P) \to \Upsilon(1S)\gamma]}{\Gamma[\chi_{b2}(3P) \to \Upsilon(1, 2, 3S)\gamma] + \Gamma[\chi_{b2}(3P) \to gg]}.$$

The radiative width can be obtained from the potential models [22,24]. Using the cross section of $\Upsilon(1S)$ produced via $\chi_{b1,2}(3P)$ radiative decays,

$$\sigma^{\mathrm{th}}[3P, 1S] = \mathrm{Br}_1[3P, 1S]\sigma_1^{\mathrm{th}}[3P] + \mathrm{Br}_2[3P, 1S]\sigma_2^{\mathrm{th}}[3P],$$

we can express the unknown branching fraction of the $\chi_{b1}(3P) \to \Upsilon(1S)\gamma$ decay through the ratio of the $3P$ and $1P$ production cross sections. The results are presented in Table III, where we denoted

$$\gamma = \frac{\sigma^{\mathrm{th}}[3P, 1S]}{\sigma^{\mathrm{th}}[1P, 1S]}.$$

So, if the experimental value of γ is found, the estimation on the radiative width $\chi_b 1(3P) \to \Upsilon(1S)\gamma$ will be found too. Similar estimations can also be performed for the $\chi_b \to \Upsilon(2S)\gamma$ processes.

IV. CONCLUSIONS

The present paper is devoted to the χ_b-meson production in hadronic experiments. Recently ATLAS [1] and D0 [2] Collaborations reported on the observation of $\chi_b(1, 2, 3P)$ states, so a theoretical description of these processes is desirable.

In our paper we use both color-singlet and color-octet models for descriptions of the P-wave heavy quarkonia production. For high energy reactions these mesons are produced mainly in gluon-gluon interactions, and the cross sections of the corresponding processes can be written as a convolution of partonic cross sections and gluon distribution functions in initial hadrons. If one uses the usual distribution functions integrated over the gluon transverse momentum and works at leading order (i.e., only $gg \to \chi_b$ partonic reactions are considered), the information about the transverse momentum distribution of final quarkonia p_T is lost. It is clear that to describe this distribution one has to use next-to-leading-order results when additional gluons in the final state are present. For high p_T values processes with an emission of additional gluons are suppressed by a small strong coupling constant, so main contributions come from reactions with a single hard gluon in the final state. For this reason we consider NLO partonic reactions $gg \to \chi_{QJ}g$. It should be noted that in this approach the production of the axial χ_1 meson is possible, while at leading order it is forbidden by Landau-Yang theorem.

In our article we discuss transverse momentum distributions of $\chi_{c,b}$ mesons. It is shown that in the case of χ_c-meson production our predictions agree well with the available experimental data. In the case of $\chi_b(nP)$ mesons, we give predictions of their p_T distributions and absolute cross sections in ATLAS and LHCb experiments. One interesting property we found is that, according to our estimations, distributions of the ratios $[d\sigma(\chi_2)/dp_T]/[d\sigma(\chi_1)/dp_T]$ for charmonium and bottomonium mesons coincide if the scaling $p_T^{\chi_b} \to (M_{\chi_c}/M_{\chi_b})p_T^{\chi_b}$ is performed. Using existing information about radial excitation of χ_b mesons from different potential models, we predict the ratio of $\chi_b(2P)$ and $\chi_b(1P)$ yields. Unfortunately, ATLAS and D0 Collaborations do not provide the information about the normalization of their results, so currently comparison with experimental data is not possible. As for the newly observed $\chi_b(3P)$ meson state, we show that from the ratios of $\chi_b(3P)$ and $\chi_b(1, 2P)$ production cross sections one can determine the branching fractions of $\chi_{b1}(3P) \to \Upsilon(1, 2S)\gamma$ decays.

ACKNOWLEDGMENTS

We would like to thank Dr. Vakhtang Kartvelishvili, Vladimir Obraztsov, and Alexey Novoselov for useful criticism. We also want to thank colleagues from the LHCb Collaboration and especially Ivan Belayev for discussions. The work was financially supported by Russian Foundation for Basic Research (Grant No. 10-02-00061a) and the grant of the president of Russian Federation (Grant No. MK-3513.2012.2).

[1] G. Aad *et al.* (ATLAS Collaboration), Phys. Rev. Lett. **108**, 152001 (2012).
[2] V. M. Abazov *et al.* (D0 Collaboration), Phys. Rev. D **86**, 031103 (2012).
[3] V. G. Kartvelishvili, A. K. Likhoded, and S. R. Slabospitsky, Sov. J. Nucl. Phys. **28**, 678 (1978).
[4] S. S. Gershtein, A. K. Likhoded, and S. R. Slabospitsky, Sov. J. Nucl. Phys. **34**, 128 (1981).

[5] L. Gribov, E. Levin, and M. Ryskin, Phys. Rep. **100**, 1 (1983).
[6] S. Catani, M. Ciafaloni, and F. Hautmann, Nucl. Phys. **B366**, 135 (1991).
[7] J. C. Collins and R. Ellis, Nucl. Phys. **B360**, 3 (1991).
[8] B. A. Kniehl, D. V. Vasin, and V. A. Saleev, Phys. Rev. D **73**, 074022 (2006).
[9] F. Abe *et al.* (CDF Collaboration), Phys. Rev. Lett. **79**, 578 (1997).
[10] R. Aaij *et al.* (LHCb Collaboration), Phys. Lett. B **714**, 215 (2012).
[11] R. Gastmans, W. Troost, and T. T. Wu, Nucl. Phys. **B291**, 731 (1987).
[12] P. L. Cho and A. K. Leibovich, Phys. Rev. D **53**, 6203 (1996).
[13] M. Klasen, B. A. Kniehl, L. N. Mihaila, and M. Steinhauser, Phys. Rev. D **68**, 034017 (2003).
[14] M. M. Meijer, J. Smith, and W. L. van Neerven, Phys. Rev. D **77**, 034014 (2008).
[15] A. Luchinsky and S. Poslavsky, Phys. Rev. D **85**, 074016 (2012).
[16] G. T. Bodwin, E. Braaten, and G. P. Lepage, Phys. Rev. D **51**, 1125 (1995).
[17] A. Abulencia *et al.* (CDF Collaboration), Phys. Rev. Lett. **98**, 232001 (2007).
[18] CMS Collaboration, Report No. CMS-PAS-BPH-11-010 (to be published).
[19] M. Kramer, Prog. Part. Nucl. Phys. **47**, 141 (2001).
[20] C. R. Munz, Nucl. Phys. **A609**, 364 (1996).
[21] D. Ebert, R. Faustov, and V. Galkin, Mod. Phys. Lett. A **18**, 601 (2003).
[22] V. Anisovich, L. Dakhno, M. Matveev, V. Nikonov, and A. Sarantsev, Phys. At. Nucl. **70**, 63 (2007).
[23] G.-L. Wang, Phys. Lett. B **674**, 172 (2009).
[24] B.-Q. Li and K.-T. Chao, Commun. Theor. Phys. **52**, 653 (2009).
[25] C.-W. Hwang and R.-S. Guo, Phys. Rev. D **82**, 034021 (2010).
[26] K. Nakamura *et al.* (Particle Data Group), J. Phys. G **37**, 075021 (2010).
[27] LHCb collaboration, Report No. CERN-LHCb-CONF-2012-020, 2012 (to be published).